EKSPLOATACJA I NIEZAWODNOŚĆ MAINTENANCE AND RELIABILITY

Eksploatacja i Niezawodnosc – Maintenance and Reliability

Volume 23 (2021), Issue 2

journal homepage: http://www.ein.org.pl

Article citation info:
Mazurkow A, Witkowski W, Kalina A, Wierzba B, Oleksy M. The effect of oil feeding type and oil grade on the oil film bearing capacity. Eksploatacja i Niezawodnosc – Maintenance and Reliability 2021; 23 (2): 381–386, http://doi.org/10.17531/ein.2021.2.18.

The effect of oil feeding type and oil grade on the oil film bearing capacity

Indexed by: Web of Science Group

Aleksander Mazurkow[a], Waldemar Witkowski[a,*], Adam Kalina[a], Bartłomiej Wierzba[a], Mariusz Oleksy[a]

[a] Rzeszów University of Technology, al. Powstańców Warszawy 8, Rzeszów, Poland

Highlights

- Oil hydrodynamic bearings can be fed from a lubrication pocket or from the face side.
- The analysis for two oil fed method and two oils were made.
- The method of oil fed and type of oil depends the bearing static characteristics.
- This study could help to chose the oil and fed method for plain bearings.

Abstract

Two types of hydrodynamically lubricated plain journal bearings were subject to examination differing in the method used to feed them with oil. The first type was fed from a lubrication pocket and the second from the bearing face side. Mathematical models were developed with two-way oil flow allowing to determine the oil film bearing capacity, the maximum pressure, the maximum temperature, and the film oil minimum height for given position of journal relative to solid bush. Static characteristics were developed used in the further course of the study to compare operating parameters of the considered types of bearings. Another issue considered in the paper is the effect of oil VG grade on bearing performance with conditions of oil feeding taken into account and results of the research presented.

Keywords

hydrodynamic bearing, oil feeding method, static characteristics, viscosity, VG oil grade, relavity eccentrity, THD.

List of basic symbols

B – bush width (m); $C_R = 0.5(D - D_J)$ – radial clearance (m); $D = 2R$ – diameter (m); e – eccentricity (m); h – oil film height (m); F – load (N); h_{min} – minimum oil clearance height (m); n_J – journal rotational speed (rpm); p – pressure in oil film (N/m^2); T – temperature (°C); $x = \varphi \cdot R$ – Cartesian system coordinate (m); y – Cartesian system coordinate (m); z – Cartesian system coordinate (m); β – journal center (O_J) and bush center (O) attitude line angle; $\varepsilon = e/C_R$ – relative eccentricity; ω_J – Journal rotational speed (rad/s). Indexes: B – solid bush; J – journal, ZC – fresh oil feeding from the bearing face side; ZK – feeding with fresh oil from a lubrication pocket.

1. Introduction

Plain bearings are commonly used in various types of machine solutions or in transmission systems. Increasingly higher requirements for bearing systems, such as high durability, operation at high rotational speeds, increasing greater thermal loads, increasing load capacity, and lowering the vibration level, require an in-depth analysis of their properties. Currently, research are conducted both of a theoretical basis - mathematical models simulating real working conditions, and experimental ones [13, 17].

One of the example are results of tests of dynamic properties of the rotor bearing system presented in [4, 6, 16, 26]. Computational simulations showed that for the new bearing concept load capacity, temperature in the oil film and fluid-induced instability conditions are dependent on the rotational speed directions. For positive rotational speed of the bearing (shaft and bearing surfaces rotate in the same directions) the average velocity of the oil film (thus, the load capacity) was increasing and viscous shear of the film (reducing oil temperature) was decreasing. For opposite directions of the bearing rotational speed the average velocity of the oil film was decreasing (avoiding fluid-induced instability) [15].

The instability of hydrodynamic bearings can be diagnosed by using Teager-Kaiser energy operator. The experimental tests were conducted for two cases of rotor unbalance: G6.3 in accordance in ISO 1940-1 [28] standard and twice greater as allowed in the ISO 1940-1 standard. In the results analyses the energy operator, measured rotor displacement and acceleration of bearing were presented in [3]. By using new analytical method for calculating the nonlinear floating ring bearings oil film the unbalance effect influencing the rotor response was presented in [20]. The engine excitation effects shown that the rotor response has a distinct difference at lower and higher speeds as well.

The angular misalignment effects on bearing performance is a very important issue. The manufacturing tolerances, installation error and elastic deflection of the rotors are the misalignment potential causes. The numerical investigation of pad tilt motion and the spherical pivot of tilt, pitch and yaw motions was presented in [10, 19]. The increasing misalignment led to the stiffened bearing and decreased minimum film thickness (increased lubricant peak temperature) [19]. The effect of the axial movement of journal on the maximum film pressure, load

(*) Corresponding author.

E-mail addresses: A. Mazurkow - almaz@prz.edu.pl, W. Witkowski - wwitkowski@prz.edu.pl, A. Kalina - akalina@prz.edu.pl, B. Wierzba - bwierzba@prz.edu.pl, M. Oleksy - molek@prz.edu.pl

capacity and over-turning moment and friction power loss is relatively weak for the small eccentricity and for the smaller the rotational speed is greater [10].

The problems associated with environmental protection can be solved with the lubrication by water. The results of research on new design solutions for this type of bearings are presented in [7]. As a result of the research, it was noticed that the turbulent flow in relation to the laminar flow increases the load bearing capacity. On the other hand, an increase of the water temperature in the bearing reduces the load capacity [7]. The influences of misalignment on the lubrication performances and lubrication regimes transition of water lubricated bearing was presented in [23]. With the increase of the misaligned angle the maximum pressure and shear stress increased, the minimum film thickness decreased and the eight dynamic coefficients increased. The micro interface lubrication regime influence on the streamline, pressure, eddy viscosity and kinetic energy distribution in the micro cavities were discussed in [24].

The transverse self-aligning hydrodynamic bearings operating in the turbine drive systems at high speeds have good hydrodynamic working stability. The influence of the oil film pressure and temperature distributions on the pads deformation was presented. Tests were conducted for static equilibrium position of the journal [5, 18]. The bearing load capacity related to each pressure distribution can be calculated by researching the dimensionless lubricant film thickness in the circumference direction. The lubricant film thickness reflects directly the bearing topology structure can be expressed by harmonic functions [25].

The results of the research on increasing the bearing capacity, reducing the coefficient of friction and wear with the use of nanofluids are presented in [1, 16]. The use of TiO_2 nanoparticles in a nanofluid for different oils (DTE 26, DTE 25, DTE 24) and different rotational speeds was investigated. Increasing the rotational speed from 500 rpm to 1500 rpm caused that the dissipation power and temperature increased around 600% and 800%, respectively [1]. The use of tungsten disulfide nanoparticles (IF-WS_2 NPs) in nanofluid increased the bearing load carrying capacity about 18% [16]. Increased load carrying capacity, significantly reduced peak pressures, more oven oil film pressure distribution and thicker oil film in the loaded zone compared to a white metal bearing can be obtained also by using PTFE layer as a bearing liner [9].

The adiabatic or diathermic theoretical models, which taking into account the influence of temperature on the oil viscosity, as shown by the research results, significantly make the temperature distribution in the oil film more accuracy to the results of experimental research [8, 14]. Concerning the ability to predict friction power losses in journal bearings, the research results indicate that the considerably simpler elastohydrodynamic approach appears to be sufficient to reliably and accurately predict these losses for full film lubrication and to investigate the occurrence of metal-metal contact [2, 21].

In many mechanical application the floating ring bearings are used instead the plain bearings [12]. But theoretical models are much more complex for that bearings. To analyze mechanical and thermal performances the thermohydrodynamic model can be used [11]. The floating ring bearings system is inherently nonlinear. If it is lightly loaded or operated at high speeds, it is prone to the fluid-induced instability. Several approaches for the linearization of the forces acting in floating ring bearings were proposed and analyzed in [6].

In industrial practice, the radial plain bearings can be feed with fresh oil from a lubrication pocket located in the non-working part of the oil film or from the face side of the bearing. In the literature and in standards [27, 13], methods for calculating the bearings operating parameters feed with fresh oil from a lubrication pocket are presented. But there are no such methods for the oil feed from the face side of the bearing. The experimental results of thermal phenomena accompanying operation of a water-lubricated stern tube bearing with axial grooves (lubricant feed from face side) were discussed in [22]. It should be noted here, that face side oil feed is a common method used for example in the bearing of crankshafts, engine timing gear, and turbochargers.

The basis of mathematical models of this type of bearings are the equations of the pressure distribution in the oil and temperature distribution in the lubricating gaps, and the equation of the oil clearance geometry. The above equations are supplemented with the equation of the mathematical model of the oil lubricating the bearing. The pressure and temperature distribution equations are differential equations that are solved for boundary conditions reflecting the actual operating conditions of the bearing [1, 14]. The boundary conditions are related to the oil feed form.

The conducted analysis of the state of knowledge has shown that the issues concerning, among others: operation and construction of slide bearings are the subject of many scientific studies. However, it should be noted that in the available literature, no studies have been found concerning plain bearings feed with oil from face side. Moreover, the available literature does not present any mathematical models to describe the lubrication of bearings with such a supply. Therefore, it was considered justified to build a mathematical model for these bearings to describe the properties of the oil film, which will be based on models intended for bearings supplied with oil from the lubricating pocket. The mathematical model was the hydrodynamic lubrication model, taking into account the influence of temperature on the oil viscosity. The static characteristic of plain bearings were developed for a better presentation of the bearing working condition. These characteristic allow for the given journal position relative to the solid bushing (ε) and type of the oil $\eta(T)$ to determine the maximum pressure (p_{max}), the maximum temperature (T_{max}), and the oil clearance minimum height (h_{min}).

Another issue, that has been considered in this manuscript, and which significantly affects on the bearing operation conditions, was the type of the oil oil viscosity used to feed the bearing. The ISO oil viscosity classification according to ISO 3448:1992 [29] was used for the tests. The obtained results allow to determine, if the oil used for plain bearing lubrication, was chosen appropriate. The maximum oil film temperature as a criterion for proper operation condition was used. The test results were presented in the form of graphs. Other parameters influencing the lubricating properties will be taken into account in further research.

2. Materials and models

2.1. Equations of mathematical model for a bearing fed from lubrication pocket

The structure, geometry, and oil flows in a bearing fed with oil from a lubrication pocket is presented in Figure 1. For the purpose of involved calculations, the method recommended in the standard [27] was used.

Similarly, the structure, geometry, and oil flows in a bearing fed from the face side are shown in Figure 2. The calculation model employed for this oil supply type was verified by means of experimental studies [13, 14].

2.2. The mathematical model constitutes a system of equations describing:

- **pressure distribution in oil clearance:**

$$\frac{4}{D^2}\frac{\partial}{\partial\phi}\left(h^3\cdot\frac{\partial p}{\partial\phi}\right)+\frac{\partial}{\partial z}\left(h^3\cdot\frac{\partial p}{\partial z}\right)=6\cdot\eta\cdot\omega_J\frac{\partial h}{\partial\phi} \tag{1}$$

Equation (1) was obtained after transformation of the equation of momentum conservation for oil particles and the equation of flow continuity [27].

- **oil clearance shape:**

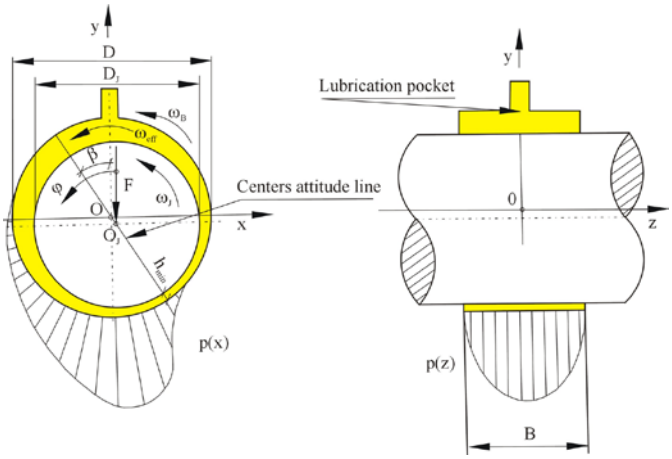

Fig. 1. The geometry, oil flow directions, and oil pressure distribution in a plain journal bearing fed with fresh oil from lubrication pocket

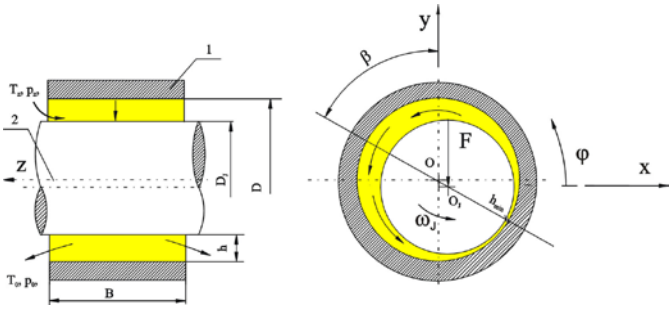

Fig. 2. The geometry, oil flow directions in case of feeding with fresh oil from the bearing face side

$$h = 0.5 \cdot D \cdot \psi_R \left[1 + \varepsilon \cdot cos(\varphi - \beta)\right] \tag{2}$$

where: $\psi_R = \frac{C_R}{D}$

Equation (2) was obtained by assuming the reference system as in Figure 1 or Figure 2 [27].

- **emperature distribution in oil clearance in case when the heat from bearing is carried away by flowing oil:**

$$\rho \cdot c_{p\cdot} \cdot \left[\upsilon_x^* \cdot \frac{\partial T}{\partial x} + \upsilon_z^* \cdot \frac{\partial T}{\partial z}\right] = \eta \cdot \left[\upsilon_x^{**} + \upsilon_z^{**}\right] \tag{3}$$

where:

$$\upsilon_x^* = \int_0^h \upsilon_x dy, \upsilon_z^* = \int_0^h \upsilon_z dy, \upsilon_x^{**} = \int_0^h \left(\frac{\partial \upsilon_x}{\partial y}\right)^2 dy, \upsilon_z^{**} = \int_0^h \left(\frac{\partial \upsilon_z}{\partial y}\right)^2 dy.$$

The equation describing the temperature distribution was derived from the energy balance equation.

- **properties of oil lubricating the bearing:**

$$\eta(T) = \eta_0 \cdot e^{a_\eta \cdot (T - T_0) + b_\eta \cdot (T - T_0)^2}, \ \rho(T) = const, \ c_p(T) = const \tag{4}$$

For the sake of the present considerations it is assumed that the oil is a Newtonian fluid [27].

In case of the bearing fed from lubrication pocket, the system of mutually adjoint equations (1–4) was solved for boundary conditions applicable to the pressure field and the temperature field. The conditions are represented in Figure 3.

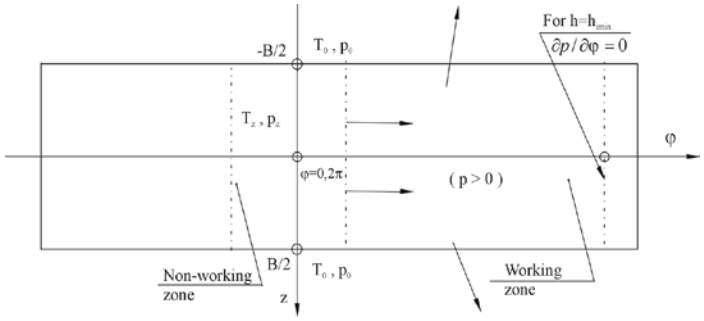

Fig. 3. Boundary conditions for pressure and temperature field in the model of bearing fed with oil from a lubrication pocket. Lines ended with arrows indicate directions of oil flow in the bearing

In case of the bearing fed with oil from its face side, the system of Equations (1–4) was solved for boundary conditions applicable to the pressure field. The conditions are presented in Figure 4.

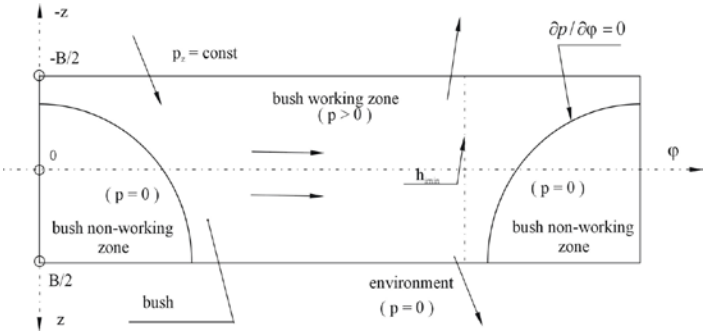

Fig. 4. The pressure field boundary conditions for a bearing fed with oil from the face side. Lines ended with arrows indicate directions of oil flow in the bearing

On the other hand, boundary conditions for the temperature field are depicted in Figure 5, where:

$$\beta_x = \frac{\eta\left(\upsilon_{xi}^{**} + \upsilon_z^{**}\right) \cdot \upsilon_{xi}^*}{\rho \cdot c_p((\upsilon_z^*)^2 + (\upsilon_{xi}^*)^2)} \quad \beta_z = \frac{\eta\left(\upsilon_{xi}^{**} + \upsilon_z^{**}\right) \cdot \upsilon_z^*}{\rho \cdot c_p((\upsilon_z^*)^2 + (\upsilon_{xi}^*)^2)} \tag{5}$$

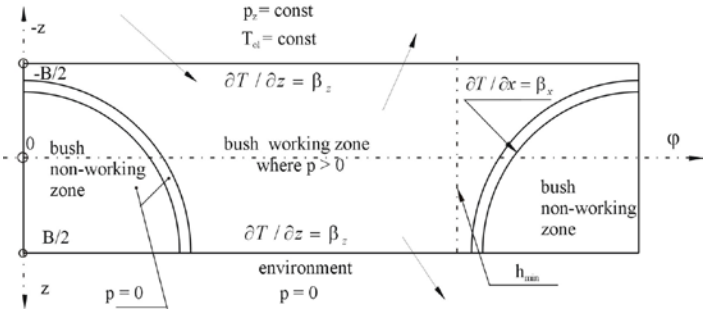

Fig. 5. The temperature field boundary conditions for a model of bearing fed with oil from the face side

The result of solving the problem of thermo-hydrodynamic equilibrium of the journal relative to the solid bush are the following quantities: $p(\phi,z), T(\phi,z), h(\phi,z), F = F_L$

3. Results

3.1. A comparative study on operating parameters of bearings fed with oil from a lubrication pocket and from the face side

For the present study, two oils have been selected with properties summarized in Table 1. The calculations were carried out for a bearing fed with oil either from lubrication pocket or from the bearing face side. As a preset quantity, position of the journal relative to the solid bush (ε) was assumed. Results of the research in the form of static characteristics as functions depending on the oil type are presented in graphical form in Figure 6.

With increasing value of ε, the minimum oil clearance height decreases. For the discussed calculation example, the condition of fluid friction is met in the whole range of considered relative eccentricity values ($h_{min} \leq h_{allow}$ =15 μm).

3.2. The effect of oil VG grade and oil feeding method on operating conditions of the bearing

In order to determine the effect of oil grade, oils of the following viscosity grades were examined: VG32, VG46, VG68, VG100, VG150. Results of tests allowing to establish the effect of oil grade and the oil feeding method are presented in graphical form as plots of the function $T_{max} = T_{max}(VG, \varepsilon, F_L$, oil feeding method). For the assumed preset values, the function takes the form shown in Figure 7.

Table 1. Preset quantities

	Preset parameters	
1.	Journal nominal diameter	D_J = 131.925 mm
2.	Solid bush nominal diameter	D = 132.109 mm
3.	Journal-floating bush relative clearance	ψ = 1.39‰
4.	Relative width	B/D = 0.5
5.	Relative eccentricity	$\varepsilon = \langle 0.2–0.85 \rangle$
6.	Journal rotational speed	ω_J= 500 s^{-1}, n_1= 4774.65 rpm
7.	Oil viscosity	$\eta_0^{(1)}$ = 0.1084 Pa·s, $a_\eta^{(1)} = -55291 \cdot 10^{-6}$, $b_\eta^{(1)} = 239 \cdot 10^{-6}$ $\eta_0^{(2)}$ = 0.5264 Pa·s, $a_\eta^{(2)} = -75000 \cdot 10^{-6}$, $b_\eta^{(2)} = 349 \cdot 10^{-6}$
8.	Oil density	ρ_0 = 900 kg/m^3
9.	Oil specific heat	c_{p0} = 2000 J/kg·°C
10.	Bearing feeding oil and environment temperature	T_z = 50°C, T_0 = 20°C
11.	Bearing feeding oil pressure	p_z = 0.1 MPa

Table 2. Bearing operating parameters

Oil feeding method	p_{allow}=15 [MPa]	
	η_0=0.1084 [Pa·s]	η_0=0.5264 [Pa·s]
Oil feeding from the bearing face side	ε^p_{allow}=0.81 T_{max}=111[°C]	ε^p_{allow}=0.75 T_{max}=124[°C]
Oil feeding from a lubrication pocket	ε^p_{allow}=0.75 T_{max}=117[°C]	ε^p_{allow}=0.71 T_{max}=130[°C]

Table 3. Operating parameters of the bearing

Oil feeding method	T_{allow} = 95°C	
	η_0 = 0.1084 Pa·s	η_0 = 0.5264 Pa·s
Oil feeding from the bearing face side	ε^T_{allow} = 0.71 F_{allow} = 23.5 kN p_{max} = 8.0 MPa	$T_{max} > T_{allow}$
Oil feeding from a lubrication pocket	ε^T_{allow} = 0.64 F_{allow} = 19.0 kN p_{max} = 7.0 MPa	$T_{max} > T_{allow}$

The relative eccentricity (Figure 6, Tables 2 and 3) determining position of the journal relative to the solid bush (ε) has an effect on fulfillment of criteria of current operation, namely: $p(\varphi,z) \leq p_{allow}$, $T(\varphi,z) \leq T_{allow}$, $h_{min} \leq h_{allow}$.

With increasing value of ε (Figure 6), value of the maximum pressure in oil film (p_{max}) increases accordingly. Adopting the allowable value of surface pressures for the bush material p_{allow} =15 MPa, values allowable for the relative eccentricity ε^p_{allow} for the lubrication pocket oil feeding method are lower than those in the case of oil being fed from the bearing face side (Figure 6, Table 2).

It follows from analysis of the course of the maximum temperature function (Figure 6) that with increasing value of ε, the maximum temperature initially decreases, and for $\varepsilon \geq 0.5$ it starts to increase. The function $T_{max} = T_{max}(\varepsilon)$ for both of the two feeding methods reaches its minimum for the value $\varepsilon^{Tmax}_{min} \approx 0.45$. Adopting T_{allow} = 95°C as the allowable oil temperature, allowable values of the relative eccentricity ε^T_{allow} , the corresponding oil film bearing capacity values ($F_{Lallow} = F_{allow}$), and maximum pressures with the feeding method taken into account the values which are presented in Table 3. For an oil with η_0 = 0.5264 Pa·s, values of the maximum temperature ($T_{max} > T_{allow}$ = 95°C) are exceeded in the whole examined range.

For the purpose of the study, two different values of the relative eccentricity ε were adopted, namely 0.45 and 0.7.

By analyzing the course of the function $T_{max} = T_{max}(\varepsilon, T_{allow}, F_L$, VG) and taking into account the fresh oil feeding method (Figure 7), a significant effect of oil VG grade and feeding method can be noted on bearing operation parameters such as the oil film bearing capacity or the maximum oil temperature.

4. Summary

Characteristics were developed allowing to determine conditions for correct operation of a bearing with oil VG grade taken into account. The effect of the oil viscosity, the oil clearance geometry, and the oil film pressure and temperature was demonstrated for two oil feeding methods.

By analyzing the research results presented in Table 3 it was found that for the same geometrical parameters, the face-fed bearings have higher bearing capacity. For the discussed structural design solution, the relative bearing capacity increase was found to be dF_{Lallow} = 18%.

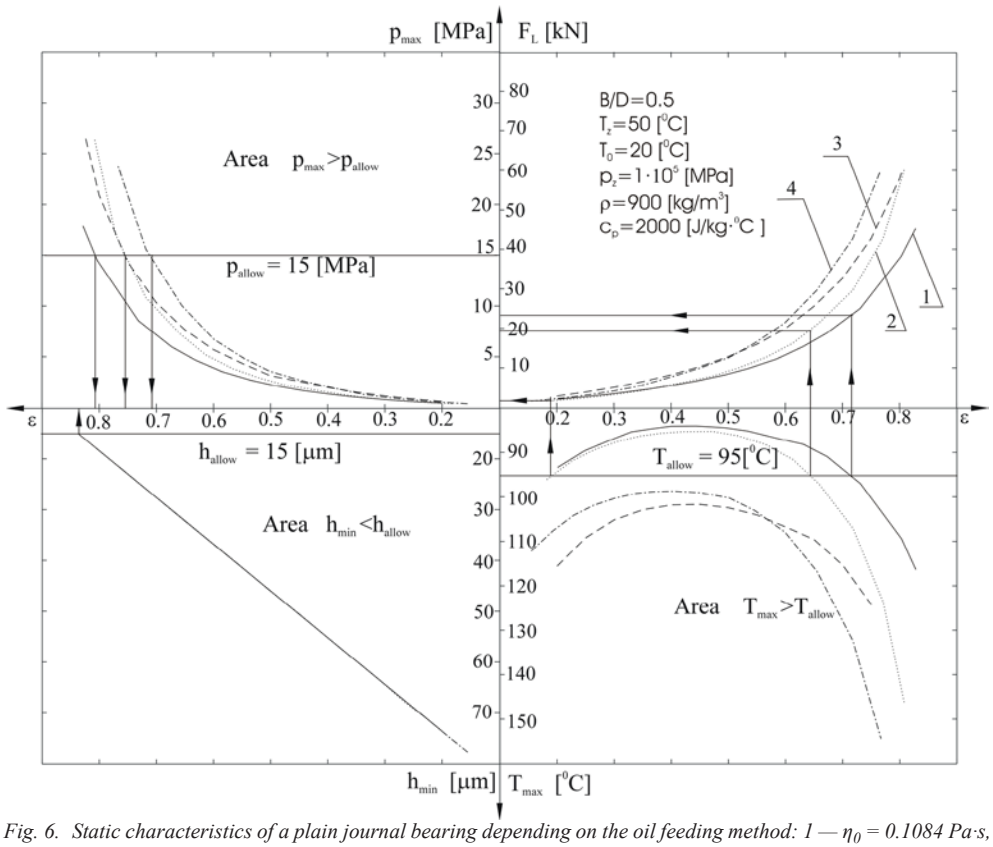

Fig. 6. Static characteristics of a plain journal bearing depending on the oil feeding method: 1 — η_0 = 0.1084 Pa·s, feeding from the bearing face side; 2 — η_0 = 0.1084 Pa·s, feeding from a lubrication pocket; 3 — η_0 = 0.5264 Pa·s, feeding from the bearing face side; 4 — η_0 = 0.5264 Pa·s, feeding from lubrication pocket

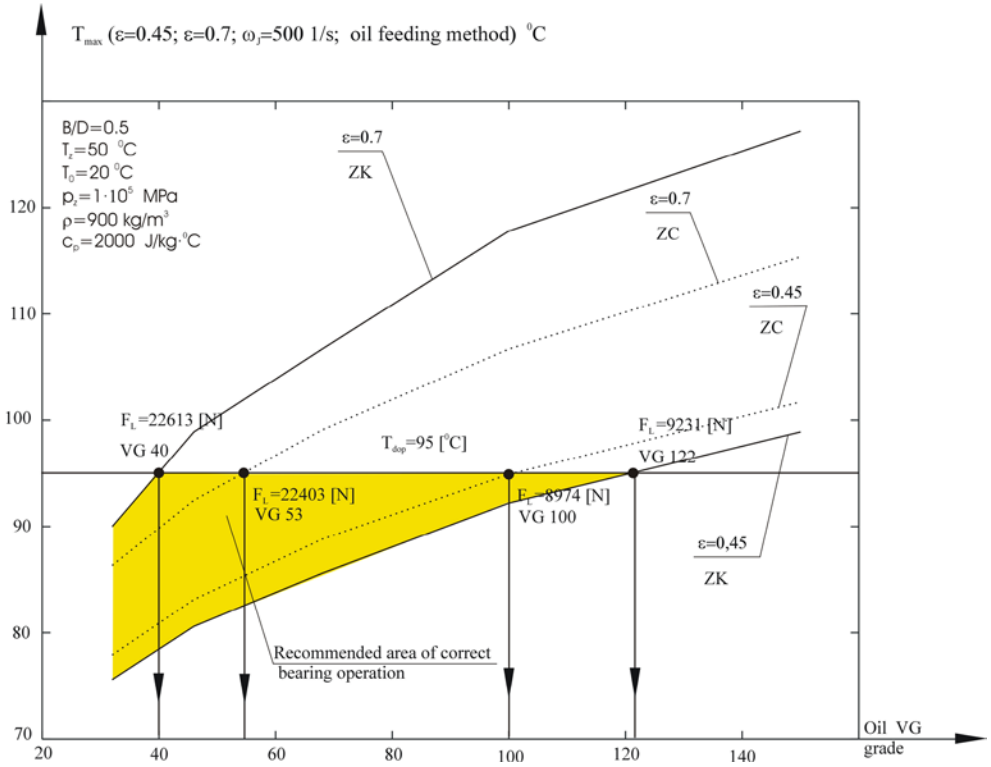

Fig. 7. The effect of oil grade on the maximum temperature in bearing. Symbols: ZC — fresh oil feeding from the bearing face side; ZK — feeding with fresh oil from a lubrication pocket

Based on research results presented in Figure 7 it can be claimed that for the eccentricity value $\varepsilon = 0.7$, bearings fed from a lubrication pocket can be operated with oils of the grade $VG_{max} = 40$, whereas oils with $VG_{max} = 53$ can be used when fed from the bearing face side. For $\varepsilon = 0.45$, the limiting grade values are $VG_{max} = 122$ and $VG_{max} = 100$, respectively.

The presented results represent the outcome of the first stage of a wider research project. In the next step, the effect of tolerance of oil operating properties on the bearing node operating parameters and dynamical properties of the bearings will be examined. The parameters influencing the lubricating properties will be also researched in the future.

References

1. Abdollahzadeh Jamalabadi MY, Alamian R, Yan W-M, Li LKB, Leveneur S, Safdari Shadloo M. Effects of Nanoparticle Enhanced Lubricant Films in Thermal Design of Plain Journal Bearings at High Reynolds Numbers. Symmetry 2019; 11(11): 1353, https://doi.org/10.3390/sym11111353.
2. Allmaier H, Priestner C, Reich F M, Priebsch H H, Novotny-Farkas F. Predicting friction reliably and accurately in journal bearings-extending the EHD simulation model to TEHD. Tribology International 2013; 58: 20-28, https://doi.org/10.1016/j.triboint.2012.08.015.
3. Blaut J, Breńkacz Ł. Application of the Teager-Kaiser energy operator in diagnostics of a hydrodynamic bearing. Eksploatacja i Niezawodnosc - Maintenance and Reliability 2020; 22 (4): 757-765, https://doi.org/10.17531/ein.2020.4.20.
4. Budzik G, Mazurkow A. Modelling and Testing of Dynamic Properties of C0-45 Turbochargers. Scientific Journal of Silesian University of Technology , Series Transport 2017; 97: 17-25, https://doi.org/10.20858/sjsutst.2017.97.2
5. Dang PV, Chatterton S, Pennacchi P. Static Characteristics of a Tilting Five-Pad Journal Bearing with an Asymmetric Geometry. Actuators 2020; 9(3): 89, https://doi.org/10.3390/act9030089.
6. Dyk S, Smolik L, Rendl J. Predictive capability of various linearization approaches for floating-ring bearings in nonlinear dynamics of turbochargers. Mechanism and Machine Theory 2020; 149: 103843, https://doi.org/10.1016/j.mechmachtheory.2020.103843.
7. Feng H, Jiang S, Ji A. Investigations of the static and dynamic characteristics of water-lubricated hydrodynamic journal bearing considering turbulent, thermohydrodynamic and misaligned effects. Tribology International 2019; 130: 245-260, https://doi.org/10.1016/j.triboint.2018.09.007.
8. Garcia M, Bou-Said B, Rocchi J, Grau G. Refrigerant foil bearing behavior-A Thermo-HydroDynamic study (Application to rigid bearings). Tribology International 2013; 65: 363-369, https://doi.org/10.1016/j.triboint.2012.12.006.
9. Kuznetsov E, Glavatskih S, Fillon M. THD analysis of compliant journal bearings considering liner deformation. Tribology International 2011; 44: 1629-1641, https://doi.org/10.1016/j.triboint.2011.05.013.
10. Li B, Sun J, Zhu S, Fu Y, Zhao X, Wang H, Teng Q, Ren Y, Li Y, Zhu G. Thermohydrodynamic lubrication analysis of misaligned journal bearing considering the axial movement of journal. Tribology International 2019; 135: 397-407, https://doi.org/10.1016/j.triboint.2019.03.031.
11. Li Y, liang F, Zhou Y, Ding S, Du F, Zhou M, Bi J, Cai Y. Numerical and experimental investigation on thermohydrodynamic performance of turbocharger rotor-bearing system. Applied Thermal Engineering 2017; 121: 27-38, https://doi.org/10.1016/j.applthermaleng.2017.04.041.
12. Mazurkow A. The design method of slide bearings with the floating ring bearing. Lap Lambert Academic Publishing, Saarbruecken, Germany, 2013, ISBN: 978-3-659-37505-7.
13. Mazurkow A. The study of journal slide bearings start-up with hydrodynamic lubrication. 55 Tribologie- Fachtagung, Gesellschaft fuer Tribologie e.V. Goettingen, 2014, ISBN: 978-3-00-046545-1.
14. Nikolic N, Antonic Z, Doric J, Ruzic D, Galambos S, Jocanovic M, Karanovic V. An Analytical Method for the Determination of Temperature Distribution in Short Journal Bearing Oil Film. Symmetry 2020; 12(4): 539, https://doi.org/10.3390/sym12040539.
15. Ramos D J, Daniel G B. A new concept of active hydrodynamic bearing for application in rotating systems. Tribology International 2021; 153: 106592, https://doi.org/10.1016/j.triboint.2020.106592.
16. Sadabadi H, Sanati Nezhad A. Nanofluids for Performance Improvement of Heavy Machinery Journal Bearings: A Simulation Study. Nanomaterials 2020; 10(11): 2120, https://doi.org/10.3390/nano10112120.
17. Santos N D S A, Roso V R, Faria M T C. Review of engine journal bearing tribology in start-stop applications. Engineering Failure Analysis 2020; 108: 104344, https://doi.org/10.1016/j.engfailanal.2019.104344.
18. Strzelecki S, Kusmierz L, Ponieważ G. Thermal deformation of pads in tilting 5-pad journal bearing. Eksploatacja i Niezawodnosc - Maintenance and Reliability 2008; 2: 12-16.
19. Suh J, Choi YS. Pivot design and angular misalignment effects on tilting pad journal bearing characteristics: Four pads for load on pad configuration. Tribology International 2016; 102: 580-599, https://doi.org/10.1016/j.triboint.2016.05.049.
20. Tian L, Wang W J, Peng Z J. Dynamic behaviours of a full floating ring bearing supportedturbocharger rotor with engine excitation. Journal of Sound and Vibration 2011; 330: 4851-4874, https://doi.org/10.1016/j.jsv.2011.04.031.
21. Wang Y, Fang X, Zhang C, Cchen X, Lu J. Lifetime prediction of self-lubricating spherical plain bearings based on physics-of-failure model and accelerated degradation test. Eksploatacja i niezawodnosc - Maintenance and Reliability 2016; 18 (4): 528-538, http://dx.doi.org/10.17531/ein.2016.4.7.
22. Wodtke M, Litwin W. Water-lubricated stern tube bearing - experimental and theoretical investigations of thermal effects. Tribology International 2021; 153: 106608, https://doi.org/10.1016/j.triboint.2020.106608.
23. Xie Z, Shen N, Zhu W, Tian W, Hao L. Theoretical and experimental investigation on the influences of misalignment on the lubrication performances and lubrication regimes transition of water lubricated bearing. Mechanical Systems and Signal Processing 2021; 149: 107211, https://doi.org/10.1016/j.ymssp.2020.107211.
24. Xie Z, Zhang Y, Zhou J, Zhu W. Theoretical and experimental research on the micro interface lubrication regime of water lubricated bearing. Mechanical Systems and Signal Processing 2021; 151: 107422, https://doi.org/10.1016/j.ymssp.2020.107422.
25. Zhang Y, Yang L, li Z, Yu L. Research on static performance of hydrodynamically lubricated thrust slider bearing based on periodic harmonic. Tribology International 2016; 95: 236-244, https://doi.org/10.1016/j.triboint.2015.11.026.
26. Zhou HL, Feng GQ, Luo GH, Ai YT, Sun D. The dynamic characteristics of a rotor supported on ball bearings with different floating ring squeeze film dampers. Mechanism and Machine Theory 2014; 80: 200-213, https://doi.org/10.1016/j.mechmachtheory.2014.04.016.
27. DIN 31652, Part 1, 2, 3. Plain bearings - Hydrodynamic plain journal bearings under steady-state conditions.
28. ISO 1940-1:2003 Mechanical vibration - Balance quality requirements for rotors in a constant (rigid) state - Part 1: Specification and verification of balance tolerances.
29. ISO 3448:1992 Industrial liquid lubricants - ISO viscosity classification.